Chinese Chemical Letters 35 (2024) 109011

Contents lists available at ScienceDirect

Chinese Chemical Letters

journal homepage: www.elsevier.com/locate/cclet

Generating electron spin qubit in metal-organic frameworks *via* spontaneous hydrolysis

Xian-Fa Jiang[a], Chongyun Shao[d], Zhongwen Ouyang[b], Zhao-Bo Hu[c,e,*], Zhenxing Wang[b,*], You Song[a,*]

[a] State Key Laboratory of Coordination Chemistry, School of Chemistry and Chemical Engineering, Nanjing University, Nanjing 210023, China
[b] Wuhan National High Magnetic Field Center & School of Physics, Huazhong University of Science and Technology, Wuhan 430074, China
[c] Chaotic Matter Science Research Center, Faculty of Materials Metallurgy and Chemistry, Jiangxi University of Science and Technology, Ganzhou 341000, China
[d] Shanghai Institute of Optics and Fine Mechanics, Chinese Academy of Sciences, Shanghai 201800, China
[e] Jiangxi Provincial Key Laboratory of Functional Molecular Materials Chemistry, Jiangxi University of Science and Technology, Ganzhou 341000, China

ARTICLE INFO

Article history:
Received 1 June 2023
Revised 3 August 2023
Accepted 28 August 2023
Available online 1 September 2023

Keywords:
Hydrolysis
Qubit
Decoherent times
Metal-organic framework
Core-shell structure

ABSTRACT

Qubit, as the basic unit of quantum operations, has at least two quantum states for superposition. Diamond itself has no superimposable quantum states, but after injecting N atoms, the resulted nitrogen-vacancy centers form excellent-performance qubits. For the same purpose, we can also obtain qubits by modifying the matrix without effective quantum states. HKUST-1 ($\{Cu_3(BTC)_2(H_2O)_3\}$, BTC = 1,3,5-benzene-tricarboxylate) with $S = 0$ ground state is electron paramagnetic resonance (EPR) silent, so it is not a qubit candidate. However, the spontaneously hydrolyzed HKUST-1 produces dilute uncoupled Cu^{II} ions with $S = 1/2$. In this paper, we utilized the hydrolysis products of HKUST-1 to obtain qubits and assembled a core-shell structural HKUST-1@ZIF-8 by ZIF-8 ($\{Zn(mim)_2\}$, mim = 2-methylimidazole) coated over HKUST-1 for controlling the hydrolysis. The experimental results clearly show that the qubits come from hydrolyzed Cu^{II} ions. Furthermore, the dilute uncoupled Cu^{II} ions in this assembly can effectively reduce the decoherence of qubits. The EPR studies show that the T_2 of this compound is 1067 ns at 10 K.

As a new computing mode, quantum computing (QC) follows the laws of quantum mechanics to manipulate the quantum states of information units [1,2]. The states of qubits, the essential units of QC, are defined by a liner combination of two computational basis state $|0\rangle$ and $|1\rangle$, termed as superposition states, different from only 0 or 1 state of classical digital bits. QC can therefore access a broader variety of states than conventional computing in a much shorter time. However, the environmental stimuli around qubit always pulls it out of its superposition states and into either the $|0\rangle$ or $|1\rangle$ state. This phenomenon, known as decoherence, seriously damages quantum coherence. So, it is necessary to prevent decoherence to avoid the loss of information over the generic state in which the qubit is, thereby allowing for more logical operations to be implemented in the time required by an algorithm. Therefore, controlling decoherence is an important topic in the qubit research. The selection of qubit carriers and their matrix are closely related to quantum decoherence. In physics, the systems based on polarized photons [3], superconductive circuits [4] and trapped ions [5] as qubits have been studied and made great progress, for example, the Sycamore and Jiuzhang photonic quantum computers reported by Google and China, respectively. In chemistry, electrons are more favored by researchers. The electron with two spin states can work as a single qubit and the electron spins can be coupled to form multilevel structures suitable for implementing complex logical operations like quantum error correction algorithms [6]. Especially, as it is easier to chemically design and synthesize, molecular spin qubits have attracted increasing attention for investigating the superposition of spin states by manipulating the electron spins with electron paramagnetic resonance (EPR) [7–13].

As regards to the synthesis of molecular spin qubits, the isolated magnetic molecules can be used to attenuate the decoherence of qubit caused by the nearby spins. The ligand field of isotropic or weak anisotropic spin carriers (such as Mn^{II} and Gd^{III} ions or Cu^{II} ion) can be regulated by the molecular symmetry to create small energy splitting within the multiplet of molecule, enabling coherent manipulation with X-band EPR [13]. Additionally, molecular qubits may be associated by the bridging ligand to design quantum gates [14]. The supramolecular approach can expand

* Corresponding authors.
E-mail addresses: huzhaobo@smail.nju.edu.cn (Z.-B. Hu), zxwang@hust.edu.cn (Z. Wang), yousong@nju.edu.cn (Y. Song).

https://doi.org/10.1016/j.cclet.2023.109011
1001-8417/

the systems to include several qubits and the bridging ligands between spin carriers can also maintain the correlation between qubits [15–19]. It indicates that the molecular design can improve the scalability of qubits. In all molecular systems, the effective spin states are the key for obtaining qubits. However, in the matrixes without spins or zero ground state spin, we can imitate the diamond nitrogen-vacancy center to produce electrons. The qubit obtained by this method is not influenced by the nearby spins, so it will show coherent properties as expected. To achieve this purpose, we choose the famous metal-organic framework (MOF) HKUST-1 ($Cu_3(BTC)_2(H_2O)_3$, BTC = 1,3,5-benzene-tricarboxylate) [20] as the candidate for qubit studies. HKUST-1 has $S = 0$ ground state with EPR silence at low temperatures. After HKUST-1 is hydrolyzed, some sites transforms into $S = 1/2$ states of Cu^{II} ions providing the chance for qubits. The phenomenon of spontaneous hydrolysis is prevalent in intricate living organisms as well, offering a means to detect the vitality of living organisms through the utilization of EPR [21,22]. In order to reduce the impact of coupling to nearby electronic spins on qubits, the core-shell nanostructures are used here. This assembly can protect HKUST-1 and prevent its further hydrolysis, ensuring a low concentration of uncoupled spin carriers in the system. The method is similar to our previous works [23,24], but the assembly products are quite different. In the previous works, trinuclear [Cu_3] clusters as the guest molecules were encapsulated in mesoporous silica or nanoporous silicon to form the host-guest compound. Thus, [Cu_3] molecules are dispersed and isolated. However in this work, another MOF, ZIF-8 ({$Zn(mim)_2$}, mim = 2-methylimidazole), is used instead of porous silica or silicon, and the compound HKUST-1@ZIF-8 with core-shell structure was prepared directly using the method in reference [25]. The synthesis process entailed the surface functionalization of HKUST-1 through the utilization of PVP, followed by the cross-linking of HKUST-1 and ZIF-8, resulting in the formation of robust chemical bonds. The adoption of this approach guarantees the enhanced stability of HKUST-1. The investigation reveals that the uncoupled spins are in a very small concentration, so the compound exhibits the relative long decoherence times (T_2) of qubits. EPR studies show that the T_2 of HKUST-1@ZIF-8 is 1067 ns at 10 K. Additionally, employing this assembly, we need not to consider the suitability of host-guest molecules, which is simpler than previous work in synthesis. This exploratory approach makes the research of molecular qubit based on core-shell structures feasible.

HKUST-1 is a three-dimensional (3D) MOF [20] in which two Cu^{II} ions are bridged by four carboxylates of BTC ligands to form a dimeric paddle-wheel unit. The dimeric units are further linked, leading to a 3D network (Fig. 1a). The carboxylates mediate strong antiferromagnetic coupling between two Cu^{II} ions with the coupling constant $J = -150 \sim -200$ cm^{-1} [26]. It implies that the ground state spin is $S = 0$, which is the main population in pure HKUST-1, especially at low temperature. So, HKUST-1 is not a qubit candidate because the excited state $S = 1$ is hard to be populated due to such a large energy gap. However, HKUST-1 is chemically unstable and its long-term exposure to moisture will promote the hydrolysis of partial Cu-O bonds in the paddle-wheels. Interestingly, the hydrolysis produces one diamagnetic Cu^{I} ion and one uncoupled Cu^{II} ion in the dimeric unit [27]. The uncoupled Cu^{II} ions in the system provide an opportunity to obtain electron spin qubits. Importantly, the hydrolysis process can be controlled by absorbing the amount of water molecules. In this way, we can achieve spin dilution in the system by controlling hydrolysis to produce a small amount of Cu^{II} monomers. The hydrolysate keeps its framework structure of HKUST-1, so the correlation between spins still exists in the 3D network with high conjugation. To prevent HKUST-1 from further hydrolysis, another MOF, ZIF-8, can be used to coat over HKUST-1, forming a compound HKUST-1@ZIF-8. Based on this strategy, the synthesis was carried out

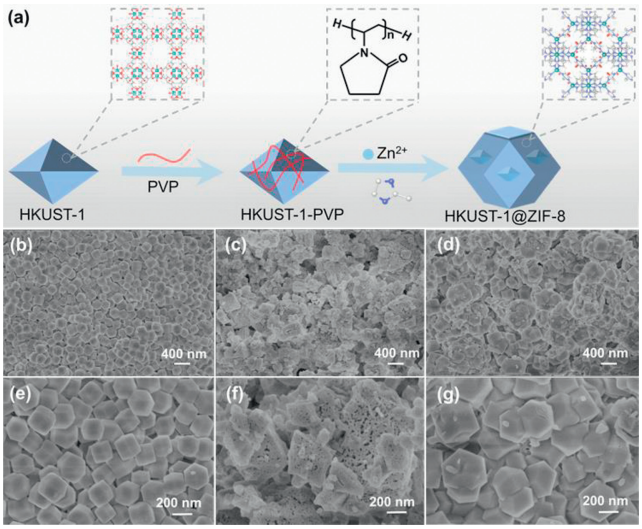

Fig. 1. (a) Schematic illustration of the fabrication process of the HKUST-1@ZIF-8. SEM images of (b) ZIF-8, (c) HKUST-1, and (d) HKUST-1@ZIF-8, whereas (e-g) are enlarged versions of (b-d), respectively.

in absolute methanol solvent and the trace amounts of water in absolute methanol participate in the hydrolysis process to control the hydrolysis products. Typically, HKUST-1@ZIF-8 was prepared by composite assembly technique (Fig. 1a). Two different MOFs, HKUST-1 and ZIF-8 (Fig. S1 in Supporting information), were effectively combined using PVP to overcome their topological mismatch. Figs. 1b and e exhibit a characteristic rhombic dodecahedron shape for ZIF-8. HKUST-1 has a distinctive octahedral form (Figs. 1c and f). Smooth and angular surfaces make it hard to detect a single HKUST-1 in the HKUST-1@ZIF-8 structure (Figs. 1d and g).

XRD reveals that HKUST-1@ZIF-8 includes all diffraction peaks expected in ZIF-8. In addition, there is a partial diffraction peak of HKUST-1, which is comprised of parts of 200 and 222 crystal planes (Fig. S2 in Supporting information). Using the N_2 adsorption/desorption curve, the specific surface areas of ZIF-8 (138.7 m^2/g), HKUST-1(608.7 m^2/g), and HKUST-1@ZIF-8 (279.6 m^2/g) can be determined. The specific surface area is, in fact, somewhere in the center, as shown by the HKUST-1@ZIF-8 comparison of the two (Fig. S3 in Supporting information). According to the TEM images, HKUST-1 has a solid octahedral interior with many small holes (Fig. S4 in Supporting information), while ZIF-8 has the form of a truncated rhombohedral dodecahedron (Fig. S5 in Supporting information). The fact that the morphologies of HKUST-1 and ZIF-8 overlap (Fig. S6 in Supporting information) indicates that the core-shell structure is established. According to chemical research of HKUST-1@ZIF-8, the C, N, O, Cu, and Zn percentages were 54.8%, 24.6%, 2.75%, 11.5%, and 6.33%, respectively (Fig. S7 in Supporting information). Through ICP analysis, the C, N, O, Cu, and Zn percentages were 53.4%, 25.1%, 2.82%, 11.9%, and 6.78%, respectively. The analysis results obtained from ICP and EDS demonstrate a similarity with the chemical compositions of HKUST-1 and ZIF-8. This is almost the same result as reported by Yang *et al.* [25].

We examine the electronic structure of HKUST-1 by using DFT theory (Fig. 2). To save computational resources, the simplest structural model of HKUST-1, namely the Cu^{II} dimer paddle-wheel building block, is used for calculation [26]. The $Cu_3(BTC)_2(H_2O)_3$ network of HKUST-1 was initially derived from the CCDC crystallographic database (No. 112954) [20]. The bond lengths and bond angles are the same as the single crystal structure besides the local unit with ligands used for building the calculated model (Fig. S8 in Supporting information) [28,29]. In this paddle-wheel

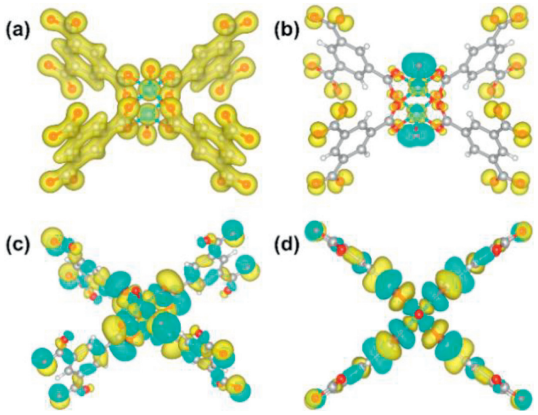

Fig. 2. The charge density (Isosurface level = 0.13), (b) spin density (Isosurface level = 0.01), (c) SOMO, and (d) SOMO-1 of HKUST-1. Color scheme: Cu, cyan; O, red; C, gray; H, white.

subunit, each copper is in a square-pyramidal environment and a water molecule in apical position. Thus, the four carboxylates each provides two oxygen atoms to two Cu^{II} ions, forming the base planes of square-pyramid and constructs the wheels, while O-Cu···Cu-O is the axle of the wheels (Fig. 2a).

The electronic structures of a complex are associated with most of its physical characteristics in some way. For example, the spin density can explain whether or how the metal ions interact with each other. Normally, the highly conjugated structure is favorable to the interaction between electrons, which may affect the qubit property of HKUST-1. However, by calculating the spin density of HKUST-1, we unexpectedly found a huge spin density on the apical water molecule (Fig. 2b), while a much lower density is obtained for the magnetic orbital of the Cu $d_{x^2-y^2}$ (Figs. 2b–d). We also tried other calculation methods [30], but the results are perfectly the same as the one above (Fig. S8). It indicates the single electrons are localized in a very small space and the magnetic properties are dominated by the paddle-wheel dimer units ($[Cu^{II}_2]$). The magnetic interaction between units is very weak. Thanks to this kind of MOF construction of HKUST-1, it is beneficial to prolong the decoherence times of the qubit in hydrolysis product, because its conjugate structure does not increase the influence of the nearby spin on qubit.

To compare the qubit property of HKUST-1 before and after hydrolysis, continuous- and pulsed-wave EPR measurements were carried out on HKUST-1 and HKUST-1@ZIF-8 (Figs. S9 and S10 in Supporting information). To obtain the signal of real HKUST-1 that is not hydrolyzed, our measuring process is very strict and the loading is all performed under the protection of inert gas. The continuous-wave (CW) spectra of HKUST-1 at 300, 100 and 4 K are shown in Fig. S8. Resonance at 300 K is smooth and unsymmetrical, which is similar to that reported by Pöppl [26] but very different from other reported results [27,31–33]. We think that it can be attributed to the purity of HKUST-1 sample. In our experiment (see Experimental part), HKUST-1 was protected carefully by dry nitrogen gas after synthesis, including all processes of removing solution, drying samples and physical measurements. At 300 K, a strong line with $S = 1/2$ is observed, which is consistent with the results in all references [26,27,31–33]. The unsymmetrical line should be from the anisotropy and the influence of nuclear spin ($I_{Cu} = 3/2$) of Cu^{II} ion. When the temperature decreases, the signal of nuclear spin is very clear at 100 K. There exists the interaction of the Cu^{II} electron spin $S = 1/2$ with its nuclear spin $I_{Cu} = 3/2$ and the hyperfine structure is observed [26,27,31]. At 4 K, the signal is almost the same as at 100 K. In all our measurements, the signal of $S = 1$ was not observed, which is attributed to the sufficiently pure sample. In contrast, the CW spectra of HKUST-1@ZIF-8 at 300 K is very broad because many signals overlap and are difficult to distinguish (Fig. S10). At 100 K, the signals become clear and show the lines of $S = 1/2$ around 3 kOe, $I_{Cu} = 3/2$ ranging from 2.5 kOe to 3 kOe and $S = 1$ at 0.12 and 4.7 kOe [27,31–33]. The signal of $S = 1$ shows the characteristics of hydrolysis products. When HKUST-1 absorbs small molecules or is hydrolyzed, the coupling strength between two 1/2 spins of paddle-wheel units is reduced significantly [27], which leads to the population of $S = 1$ state based on the antiferromagnetic coupling in a large range of temperature. However, at very low temperature such as 4 K, the population distribution of $S = 1$ state will largely decrease, so the corresponding lines disappear (Fig. S10). Since the Cu^{II} monomers as the hydrolysis products after HKUST-1 is wrapped by ZIF-8, the compound only exhibits the paramagnetic state of $S = 1/2$, resulting in a much narrower peak width for HKUST-1@ZIF-8 of the uniform distribution of paramagnetic centers. At this temperature, the best fitting results gave $g_x = g_y = 2.052$, $g_z = 2.249$, $A_x = A_y = 0.0014$ cm^{-1} and $A_z = 0.0166$ cm^{-1}. The hydrolytically paddle-wheel units can be calculated very roughly from the spin values of EPR spectra. The hydrolyzed units are near 0.05% in mole rate in HKUST-1@ZIF-8 by the spin difference of HKUST-1 (2.61×10^{-4} spin/mol) and compound (0.23×10^{-4} spin/mol) based on EPR data at 100 K. The data at 300 K cannot be used for calculation because of the ugly curves. It is believed that the real number of Cu^{II} monomers is higher than the calculation. The error in estimating spin values using EPR spectra is significant.

A Hahn echo sequence ($\pi/2$-τ-π-τ-echo) was used at $H = 3200$ Oe, $T = 4.0$ K, and $v = 9.3$ GHz (Fig. 3 and Fig. S11 in Supporting information). The field at 3200 Oe for both HKUST-1 and core-shell compound is applied in the measurement ascribed to the strong echo-detected-field-scan (EDFS) response of two compounds in this field (Fig. S10). A single exponent function was used to model the decline of echo intensity. As shown in Fig. 3a, the T_2 of HKUST-1 at 4 K is 266 ns, but the T_2 of HKUST-1@ZIF-8 is 734 ns, which is approximately three times longer than that of HKUST-1. This indicates that the spins in skeleton of HKUST-1 are not good qubit candidate as expected possibly because of the coupling limitation between Cu^{II} ions in paddle-wheel units. Yet the spins of Cu^{II} monomers are much better. It is believed that the weak coherence of HKUST-1 results from the structural defect rather than the hydrolysis product, such as the crystalline surface, which has the Cu^{II} ions with different coordinating environment from the real structure. Additionally, the decoherent time of 266 ns is much shorter than that for core-shell structure in following description, indicating the signal source is different from the hydrolysis product of HKUST-1@ZIF-8. Fig. 3b shows the echo area as a function of 2τ for HKUST-1@ZIF-8 at different temperatures, whereas Fig. 3c depicts the T_2 of HKUST-1 and HKUST-1@ZIF-8. The considerable increase in T_2 of HKUST-1@ZIF-8 over HKUST-1 results from two factors. One, also the main factor, is that the uncoupled Cu^{II} ions as the hydrolyzed product is self-diluted and the concentration is low. Thus, the qubits will not be influenced by nearby spins. The other one is that the fragments of HKUST-1 are separated in ZIF-8 and the interaction of electron spins between fragments is diminished or even eliminated [23,24,33,34]. Furthermore, when the temperature rises, the T_2 of HKUST-1@ZIF-8 climbs up and subsequently decreases with a maximum of 1067 ns at 10 K. This is commonly observed in literature [35–39], which could be due to the method of fitting the relaxation data. In Fig. 3b, in addition to the electron spin relaxation of Cu ion, the curve also contains the modulations due to the hyperfine interaction of Cu ion itself and superhyperfine interactions of the neighboring Cu ion and other atoms. Especially at low temperature, the modulation of hyperfine and superhyperfine interactions is much stronger. This kind modulation in our compounds is too complicated to be simulated for

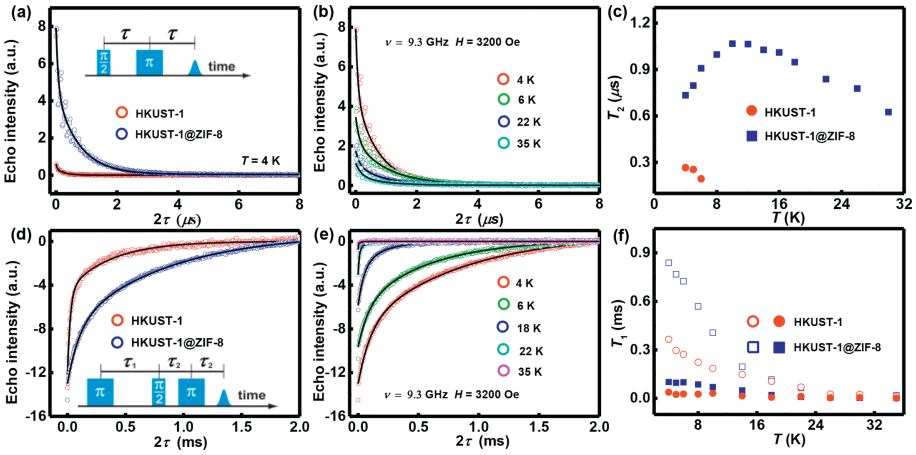

Fig. 3. Relaxation data of HKUST-1 and HKUST-1@ZIF-8 at $\nu = 9.3$ GHz and $H = 3240$ Oe. (a, b) Hahn echo experiments (open circles) with single exponent fits (solid lines). (d, e) Inversion recovery experiments (open circles) with biexponential fits (solid lines). (c, f) Dependence of T_2 and T_1 on temperature for HKUST-1 and HKUST-1@ZIF-8.

detailed analysis. For a better illustration, we normalized the data in Figs. 3a and b as shown in Fig. S11, from which it is seen that the relaxation rate of HKUST-1 is faster than that of HKUST-1@ZIF-8. The T_2 at 6 K is longer than those at other temperatures.

The spin-lattice relaxation time (T_1) was calculated by an inversion recovery sequence (π-τ_1-$\pi/2$-τ_2-π-τ_2-echo). Maps illustrating the temperature dependence of T_1 with two values given throughout the temperature range of 4–30 K can be generated using the bi-exponential decay rate observed in the echo area (Figs. 3d–f). The narrow excitation bandwidth of the microwave pulse means that it can only excite a fraction of the whole spectrum, indicating that rapid spectral diffusion leads to the short T_1. In contrast, the prolonged T_1 should correspond to the actual spin-lattice relaxation time [23,24]. As shown in Fig. 3f, T_1 becomes longer while encapsulating HKUST-1 in ZIF-8. When ZIF-8 is layered on the surface of HKUST-1, HKUST-1 fragment molecules are bound to the carrier ZIF-8, which may enhance their structural rigidity, resulting in a prolonged T_1 value. In addition, not every Cu^{II} dimeric unit undergoes hydrolysis due to trace water in the synthesis, so the effective distance between Cu^{II} ions is long enough. This approach is similar to prolonging the relaxation time of single-molecule magnets.

Investigations of spin nutation on HKUST-1 and HKUST-1@ZIF-8 at different microwave power levels reveal the coherent spin manipulation. As expected, Fig. 4 demonstrates the presence of Rabi oscillations in both HKUST-1 and HKUST-1@ZIF-8, with the frequency of these oscillations (R) being linearly dependent on microwave attenuation. Figs. 4a and c demonstrate that the peak of the electron spin signal drops progressively during cyclic coherent manipulation as a result of environmental interactions. Despite having almost no signal, HKUST-1 exhibits Rabi oscillations, indicating that HKUST-1@ZIF-8 is more susceptible to coherent manipulation than HKUST-1. To further illustrate that HKUST-1 and HKUST-1@ZIF-8 can be manipulated, spin nutation experiments were carried out at different temperatures. As expected, the existence of Rabi oscillations permits coherent control over both HKUST-1 and HKUST-1@ZIF-8. Figs. S12 and S13 (Supporting information) indicate that the Rabi oscillations in HKUST-1@ZIF-8 were much longer than in HKUST-1, and the latter was more difficult to manipulated. By assembling ZIF-8 with HKUST-1 molecules, the nutation experiment reveals the viability of building a one-qubit NOT gate for quantum computing.

In summary, with PVP as the connecting agent, the two MOFs of HKUST-1 and ZIF-8 are linked to form a compound

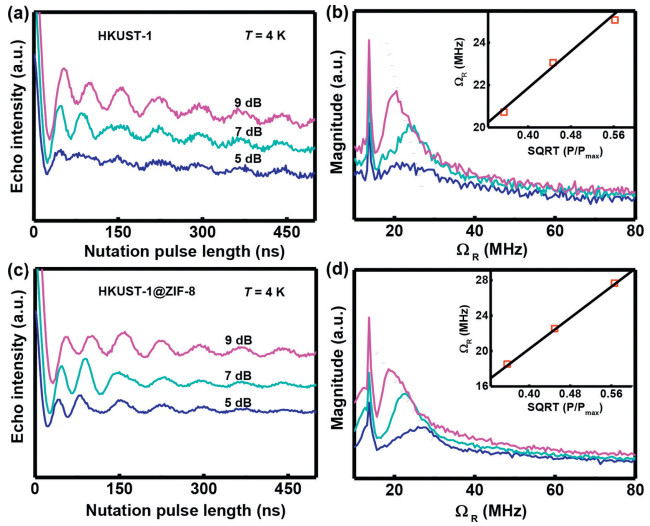

Fig. 4. Rabi oscillations were measured at 4 K for (a) HKUST-1 and (c) HKUST-1@ZIF-8 with various microwave attenuations. The Fourier transforms of (b) HKUST-1 and (d) HKUST-1@ZIF-8 of the Rabi oscillations.

HKUST-1@ZIF-8. Analyses using SEM and TEM demonstrated that ZIF-8 fully enclosed HKUST-1, thereby protecting HKUST-1. The spins of HKUST-1 enclosed in ZIF-8 are effectively controlled by fragmentation and partial hydrolysis, further the qubit coherent times with $T_2 = 1067$ ns at 10 K is observed according to EPR experiments. We have extended our work in investigating molecular qubit by host-guest chemistry through core-shell structure, and for the first time have produced guest molecules on the inner surface of modified host molecules to alter their qubit properties. Furthermore, we clearly explain the origin of qubits in HKUST-1@ZIF-8. This study provides a new strategy to obtain molecular qubits. This exploratory approach makes the research of molecular qubit based on core-shell structure (host-guest chemistry) feasible.

Declaration of competing interest

We declare that they have no known competing financial interests or personal relationships that could have appeared to influence the work reported in this paper.

Acknowledgments

This work was supported by the National Key Research and Development Program of China (No. 2021YFA1600304), the Joint Fund for Regional Innovation and Development (No. U20A2073), the National Natural Science Foundation of China (Nos. 21973038, 62005297 and 22105089), the Interdisciplinary Program of Wuhan National High Magnetic Field Center (No. WHMFC202133), Natural Science Foundation of Jiangxi Province (No. 20224BAB214005) and Jiangxi Provincial Key Laboratory of Functional Molecular Materials Chemistry (No. 20212BCD42018). We are grateful to the High Performance Computing Centre of Nanjing University for providing the IBM Blade cluster system. A portion of EPR spectroscopy spectra were measured on Chinainstru&Quantumtech (Hefei) EPR100 with X-band frequency and on the Steady High Magnetic Field Facilities, High Magnetic Field Laboratory, CAS. We thank Zhifu Shi of Chinainstru&Quantumtech for the helpful discussion and EPR spectrum measuring.

References

[1] V. Marx, Nat. Methods 18 (2021) 715–719.
[2] M.A. Nielsen, I.L. Chuang, Quantum Computation and Quantum Information, Cambridge University Press, Cambridge, 2000, p. 676.
[3] E. Knill, R. Laflamme, G.J. Milburn, Nature 409 (2001) 46–52.
[4] J. Clarke, F.K. Wilhelm, Nature 453 (2008) 1031–1042.
[5] R. Blatt, D. Wineland, Nature 453 (2008) 1008–1015.
[6] M.N. Leuenberger, D. Loss, Nature 410 (2001) 789–793.
[7] M. Atzori, R. Sessoli, J. Am. Chem. Soc. 141 (2019) 11339–11352.
[8] Y.S. Ding, Y.F. Deng, Y.Z. Zheng, Magnetochemistry 2 (2016) 40.
[9] F. Troiani, M. Affronte, Chem. Soc. Rev. 40 (2011) 3119–3129.
[10] E. Moreno-Pineda, C. Godfrin, F. Balestro, W. Wernsdorfer, M. Ruben, Chem. Soc. Rev. 47 (2018) 501–513.
[11] S. Bertaina, S. Gambarelli, T. Mitra, et al., Nature 453 (2008) 203–207.
[12] S. Hill, R.S. Edwards, N. Aliaga-Alcalde, G. Christou, Science 302 (2003) 1015–1018.
[13] E. Coronado, Nat. Rev. Mater. 5 (2020) 87–104.
[14] A. Gaita-Ariño, F. Luis, S. Hill, E. Coronado, Nat. Chem. 11 (2019) 301–309.
[15] T. Yamabayashi, M. Atzori, L. Tesi, et al., J. Am. Chem. Soc. 140 (2018) 12090–12101.
[16] A. Urtizberea, E. Natividad, P.J. Alonso, et al., Adv. Funct. Mater. 28 (2018) 1801695.
[17] C.J. Yu, M.D. Krzyaniak, M.S. Fataftah, M.R. Wasielewski, D.E. Freedman, Chem. Sci. 10 (2019) 1702–1708.
[18] L. Sun, L. Yang, J.H. Dou, et al., J. Am. Chem. Soc. 114 (2022) 19008–19016.
[19] A.K. Oanta, K.A. Collins, A.M. Evans, et al., J. Am. Chem. Soc. 145 (2023) 689–696.
[20] S.S.Y. Chui, S.M.F. Lo, J.P.H. Charmant, A.G. Orpen, I.D. Williams, Science 283 (1999) 1148–1150.
[21] M. Scarpellini, A. Neves, R. Hörner, et al., Inorg. Chem. 42 (2003) 8353–8365.
[22] N. Cetinbas, M.I. Webb, J.A. Dubland, C.J. Walsby, J. Biol. Inorg. Chem. 15 (2010) 131–145.
[23] K.Y. Choi, Z. Wang, H. Nojiri, et al., Phys. Rev. Lett. 108 (2012) 067206.
[24] X.F. Jiang, Z.B. Hu, C. Shao, et al., Chem. Mater. 34 (2022) 8427–8436.
[25] J. Yang, H. Ye, F. Zhao, B. Zeng, ACS Appl. Mater. Interfaces 8 (2016) 20407–20414.
[26] A. Pöppl, S. Kunz, D. Himsl, M. Hartmann, J. Phys. Chem. C 112 (2008) 2678–2684.
[27] M. Todaro, G. Buscarino, L. Sciortino, et al., J. Phys. Chem. C 120 (2016) 12879–12889.
[28] S. Friedländer, P. St. Petkov, F. Bolling, et al., J. Phys. Chem. C 120 (2016) 27399–27411.
[29] B. Lukose, B. Supronowicz, P.St. Petkov, et al., Phys. Status Solidi B 249 (2012) 335–342.
[30] K.A.H. Alzahrani, R.J. Deeth, Dalton Trans. 45 (2016) 11944–11948.
[31] M. Šimėnas, M. Kobalz, M. Mendt, et al., J. Phys. Chem. C 119 (2015) 4898–4907.
[32] A. Terracina, M. Todaro, M. Mazaj, et al., J. Phys. Chem. C 123 (2019) 1730–1741.
[33] M. Mazaj, T. Čendak, G. Buscarino, M. Todaro, N.Z. Logar, J. Mater. Chem. A 5 (2017) 22305–22315.
[34] Z. Liu, B.W. Dong, H.B. Meng, et al., Chem. Sci. 9 (2018) 457–462.
[35] M.S. Fataftah, M.D. Krzyaniak, B. Vlaisavljevich, et al., Chem. Sci. 10 (2019) 6707–6714.
[36] S. von Kugelgen, M.D. Krzyaniak, M.Q. Gu, et al., J. Am. Chem. Soc. 143 (2021) 8069–8077.
[37] M.J. Amdur, K.R. Mullin, M.J. Waters, et al., Chem. Sci. 13 (2022) 7034–7045.
[38] F. Luis, P.J. Alonso, O. Roubeau, et al., Commun. Chem. 3 (2020) 176.
[39] R.B. Zaripov, Y.E. Kandrashkin, K.M. Salikhov, et al., Nanoscale 12 (2020) 20513–20521.